Distribution and cycling of total organic carbon across the Almeria-Oran Front in the Mediterranean Sea: Implications for carbon cycling in the western basin

Richard Sempere, Evgeny V. Dafner, France van Wambeke, Dominique Lefèvre, Cédric Magen, Sophie Allègre, Fabienne Bruyant, Micheline Bianchi, Louis Prieur

Distribution and cycling of total organic carbon across the Almeria-Oran Front in the Mediterranean Sea: Implications for carbon cycling in the western basin

Richard Sempéré,[1] Evgeny Dafner,[1,2] France Van Wambeke,[1] Dominique Lefèvre,[3] Cédric Magen,[1,4] Sophie Allègre,[1] Flavienne Bruyant,[5] Micheline Bianchi,[1] and Louis Prieur[5]

Received 13 May 2002; revised 30 July 2003; accepted 27 August 2003; published 25 November 2003.

[1] The dynamics of the total organic carbon (TOC) pool were studied during winter 1997–1998 in the Almeria-Oran jet-front (AOF) system. This system includes the modified Atlantic Jet, which spreads into the Mediterranean Sea from the Gibraltar Strait, its associated gyre, and the front between the Mediterranean and Atlantic waters. We determined TOC concentrations, bacterial production (BP), and primary production (PP) during field work, and labile dissolved organic carbon (l-DOC) and bacterial growth efficiency (BGE), which were calculated from biodegradation experiments. Our results showed that the geostrophic Atlantic Jet, which is the most dynamic area (horizontal speed of 80 cm s^{-1} in the upper 100 m flowing eastward), was characterized by low TOC stocks integrated in the first 100 m (6330–6990 mmol C m^{-2}), a proportion of l-DOC of 5 ± 0.5%, a BGE of 15 ± 2% and moderate residence times of excess-TOC (42 ± 7 days). Higher TOC stocks were found in the surrounding areas, including the Mediterranean (7298–7400 mmol C m^{-2}) and gyre waters (6718–8315 mmol C m^{-2}) whereas l-DOC averaged 6 ± 0.9% and 15 ± 2%, respectively. BGE averaged 7 ± 1% in Mediterranean waters and 21 ± 3% in the gyre giving rise to slightly different excess-TOC residence times (28 ± 1 days in Mediterranean waters and 109 ± 30 days in the gyre). We estimated that the transport of TOC and excess-TOC within the Atlantic Jet averaged 8.04 ± 0.32 × 10^4 and 1.68 ± 0.32 × 10^4 mol C s^{-1}, respectively. *INDEX TERMS:* 4805 Oceanography: Biological and Chemical: Biogeochemical cycles (1615); 4528 Oceanography: Physical: Fronts and jets; 4803 Oceanography: Biological and Chemical: Bacteria; 4806 Oceanography: Biological and Chemical: Carbon cycling; 4815 Oceanography: Biological and Chemical: Ecosystems, structure and dynamics; *KEYWORDS:* total organic carbon, bacteria, carbon cycling, front and jet, Mediterranean Sea

Citation: Sempéré, R., E. Dafner, F. Van Wambeke, D. Lefèvre, C. Magen, S. Allègre, F. Bruyant, M. Bianchi, and L. Prieur, Distribution and cycling of total organic carbon across the Almeria-Oran Front in the Mediterranean Sea: Implications for carbon cycling in the western basin, *J. Geophys. Res.*, *108*(C11), 3361, doi:10.1029/2002JC001475, 2003.

1. Introduction

[2] In oceanic waters, dissolved organic carbon (DOC), which accounts for most of the total organic carbon (TOC) stock is the result of the imbalance between the inputs and outputs, of in situ biological production and consumption processes [*Anderson and Williams*, 1999; *Carlson*, 2001; *Hansell*, 2001, and references therein]. Previous studies in the Mediterranean basin have shown that the main external source of organic carbon was Atlantic water spreading through the Gibraltar Strait [*Copin-Montégut*, 1993; *Dafner et al.*, 2001a, 2001b], this is followed by the contribution by rivers [*Ludwig et al.*, 1998; *Sempéré et al.*, 2000], atmospheric deposition [*Loïe-Pillot et al.*, 1992] and finally the Black Sea [*Polat and Tugrul*, 1996; *Sempéré et al.*, 2002]. However, there are no reports which deal with the distribution and mineralization of DOC by bacteria in the Atlantic waters spreading in the Alboran Sea (southwestern Mediterranean) where further mixing takes place along with transportation eastward. Such a study could help estimate the quantity of CO_2 produced through bacterial respiration and lead to a better understanding of the carbon cycle in the Mediterranean Sea.

[3] The mixing of the strong jet of incoming Atlantic water (~1.0 Sv; 1 Sv = 10^6 m^3 s^{-1}) with the more saline

[1]Laboratoire de Microbiologie Marine, Centre d'Océanologie de Marseille, Université de la Mediterranée, Campus de Luminy, Marseille, France.
[2]Now at School of Ocean and Earth Science and Technology, University of Hawaii, Honolulu, Hawaii, USA.
[3]Laboratoire d'Océanologie Biologique, Centre d'Océanologie de Marseille, Université de la Mediterranée, Campus de Luminy, Marseille, France.
[4]Now at Sciences, Université McGill, Montréal, Québec, Canada.
[5]Laboratoire d'Océanographie de Villefranche, Observatoire Océanologique, Villefranche-sur-Mer, France.

0148-0227/03/2002JC001475

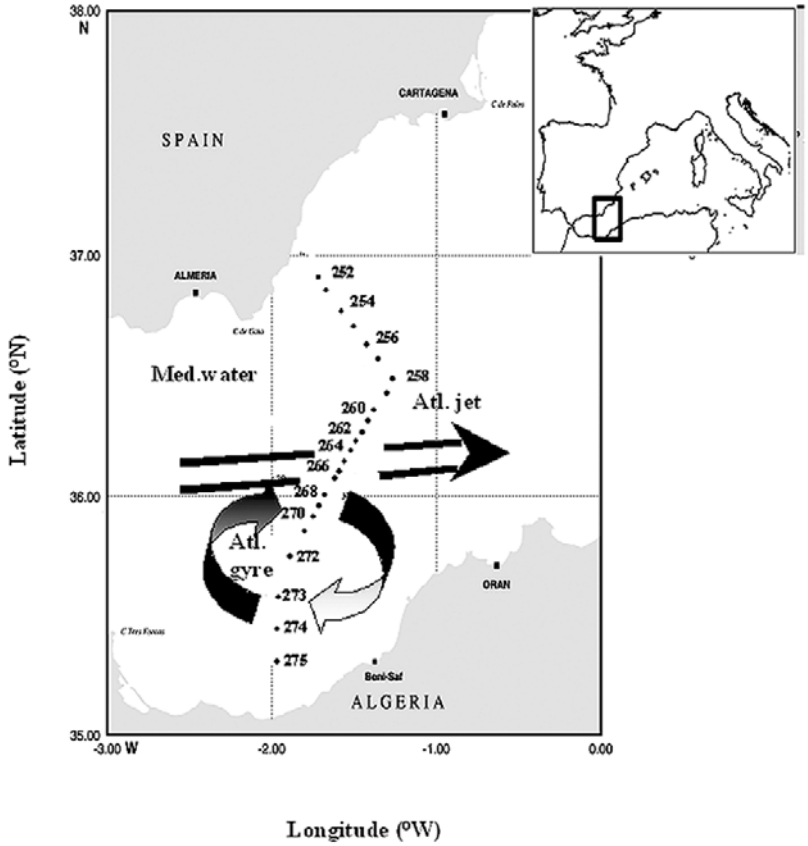

Figure 1. Map of the Alboran Sea in the southwestern Mediterranean Sea with locations of the sampling stations studied between 17 November and 21 December 1997 investigated during Almofront II program. Stations were sampled along a transect starting at station 252 (254 for TOC) near the Spanish coast and ending at station 275 near the Algerian. The arrows schematically describe the Atlantic Jet and the associated gyre.

Mediterranean water results in the formation of a geostrophic front (hereinafter Almeria-Oran front, AOF). Boundaries between different water masses are seen as sharp changes in physical structure. This can be observed during oceanographic cruises and from satellite-derived parameters including sea surface temperature (SST) and chlorophyll *a* [*Baldacci et al.*, 2001]. The incoming flow generates a quasi permanent anticyclonic gyre (Atlantic anticyclonic gyre) adjacent to the Gibraltar Strait and a less permanent gyre at the eastern part of the basin [*La Violette*, 1990; *Arnone et al.*, 1990; *Vazquez-Cuervo et al.*, 1996].

[4] The front, which is associated with the main current; that is, the Atlantic Jet (primary circulation) has a vertical circulation across the jet (secondary circulation [*Prieur and Sournia*, 1994]). It is associated with high phytoplankton standing stocks and production, which is in contrast to the two adjacent oligotrophic-type systems [*Lohrenz et al.*, 1988; *Tintoré et al.*, 1988; *Prieur et al.*, 1993; *Videau et al.*, 1994]. The high-velocity jets characteristic (up to 1 m s^{-1}) makes this area subject to intense mesoscale and subsurface variability [*La Violette*, 1990], which affects the specific composition of the autotrophic [*Claustre et al.*, 1994] and heterotrophic communities [*Fernandez et al.*, 1994; *Thibault et al.*, 1994; *Youssara and Gaudy*, 2001], the planktonic bioluminescence [*Cussatlegras et al.*, 2001], the colored dissolved organic [*Claustre et al.*, 2000] and colloidal matter [*Grout et al.*, 2001].

[5] Results are presented from a winter section across the AOF, from Almeria to Oran, which assesses for the first time the spatial dynamics of total organic carbon (TOC) in this area. The aim of the paper is to describe the distribution of TOC and its cycling by bacterioplankton in the different water masses, which are associated with the AOF, and evaluate its contribution to the carbon cycle in the western Mediterranean Sea carbon cycle. By using geostrophic transport through the eastern part of the Alboran Sea, we propose an estimate for the average TOC transport in the AOF.

2. Materials and Methods

2.1. Field Sampling

[6] This study was conducted during the first leg of the Almofront program on board RV *L'Atalante* (Figure 1) in the eastern part of the Alboran Sea over one cruise (29 November to 21 December 1997). Leg 1 focused on the hydrological and biogeochemical parameters and the position of the jet-gyre system using vessel-mounted acoustic Doppler current profilers (ADCP), intensive CTD (conductivity-temperature-depth) casts, and TOW-YO transects along a cross-frontal section (Figure 1) with stations spaced at an average distance of 11 km in the

Table 1. TOC Inventory (in mmol C m^{-2}) and Excess-TOC to TOC Ratios (%) in the Alboran Sea, Calculated From Seawater Samples Collected Along a Transect (17 November to 21 December 1997)[a]

Leg 1 Station Number	TOC, mmol C m^{-2}	Excess-TOC, %	Identification of Stations
254	7298	27 ± 3	Mediterranean water
259	7343	28 ± 3	
260	7400	28 ± 2	
261	7355	28 ± 2	
262	6850	23 ± 3	Atlantic Jet
263	6668	21 ± 3	
264	6330	16 ± 3	
265	6990	24 ± 3	
266	6853	23 ± 3	
267	8315	36 ± 2	northern gyre
268	7718	31 ± 2	
269	7315	28 ± 3	
270	6740	21 ± 3	central gyre
272	6718	21 ± 3	
273	7340	28 ± 3	
274	7980	34 ± 2	southern gyre
275	7078	25 ± 3	

[a]Excess-TOC was calculated as the integration (0–100 m) of the difference between discrete TOC data at each depth and a mean TOC value between 400 and 1000 m of 53 μM C. SE of excess-TOC was calculated by considering the standard deviation obtained for refractory DOC.

AOF area. Leg 2 ''long stations'' were studied over 36 hours for biogeochemical processes at eight sites, which were located on the AOF system at similar positions to the stations studied during leg 1. Leg 2 results relate mainly to bacterial controls and grazing and are presented by *Van Wambeke et al.* [2003].

[7] Surface salinity and temperature were measured with a thermosalinograph SBE 21 and current data was recorded using two 300-kHz and 75-kHz vessel-mounted RDI ADCP. The latter data was georeferenced and averaged over 2 and 5 min, respectively, corresponding to approximately 200 pings. Absolute velocities were determined from the ships position given by the precise differential (70 cm) global positioning system every 2 min. Geostrophic velocities and transport were derived from CTD data using 500 dbars as the point of no motion. Data from the 75-kHz ADCP confirmed the flow was less than 1 cm s^{-1} at this depth.

[8] For TOC determination, discrete seawater samples were collected at 17 stations crossing the AOF (Figure 1; Table 1) using a Seabird SBE 9 CTD carrousel sampler equipped with 24 12-L Niskin bottles. Discrete seawater samples were also collected at three stations typical of the Mediterranean, Front, and Atlantic waters during leg 1 for bacterial production (BP), primary production (PP), and for DOC biodegradation experiments.

[9] At the beginning of the cruise, Niskin bottles were cleaned with 0.2% HCl and rinsed with distilled water. Plastic O-rings were replaced by Viton material and the original plastic ribbons replaced by steel springs in order to minimize organic contamination. Vials and bottles were rinsed three times with seawater before filling with samples. For TOC determination, samples were drawn as soon as the rosette sampler was on the deck of the ship (before any other sampling) in duplicate in precombusted (450°C, at least 6 hours) 10-mL glass vials. Samples were not filtered thus by definition these are TOC and not DOC samples. Under a laminar flow airbench, samples were poisoned immediately with $HgCl_2$ (10 mg L^{-1} final concentration), and vials were closed with Teflon lined screw caps. Samples were stored in the dark and analyzed within 6 months. It has been shown recently [*Sempéré et al.*, 2002] that storage of seawater in pre-combusted glass vials closed with Teflon lined screw caps can give rise to higher TOC concentrations (5 ± 3 μM C) than seawater stored in flame-sealed ampoules. For the determination of BP, 500-mL samples were drawn into dark polycarbonate bottles. Seawater for biodegradation experiments was collected in 10-L glass bottles using Teflon tubing and was immediately processed in a temperature controlled laboratory on board. For PP determination, 700-mL samples were collected in dark glass bottles and processed immediately aboard (see below) for determination of P versus I curves.

2.2. HTCO Analysis

[10] The Shimadzu instrument used in this study is the commercially available model TOC-5000 Total Carbon Analyzer with a quartz combustion column filled with 1.2% Pt on silica pillows with an approximate diameter of 2 mm [*Cauwet*, 1994]. Several aspects of our modified unit have been previously described [*Dafner et al.*, 1999, 2001a, 2001b; *Sempéré et al.*, 2002]. Briefly, the furnace temperature was maintained at 680°C and the effluents passed through a mercury trap consisting of gold wire in order to remove mercury [*Ogawa and Ogura*, 1992]. A magnesium perchlorate water trap was added to the system situated before the halogen scrubber, the in-line membrane filter, and the non-dispersive infrared CO_2 detector. Prior to analysis, subsamples were acidified with 10 μl of 85% H_3PO_4 to pH ~2 and sparged for 10 min with CO_2-free pure air at a flow rate of 40 mL min^{-1} to remove inorganic carbon as CO_2. TOC contamination from the preservation reagent and from H_3PO_4 was below the detection limit. Injections of 100 μl were repeated 2–4 times for each sample, the analytical precision of the procedure being within 3%, on average. Some variability arise in values taken from two different vials and gives rise to a lower overall precision (8%).

[11] In order to lower the blank, the catalyst was washed in 1% HCl, gently rinsed with Milli-Q water, and dried in a furnace at 450°C for 10–15 min. Prior to the analyses of standards and samples, the catalyst bed was 'conditioned' (over 2–4 days) by injecting 100 μl of sparged acidified water from a high-quality water purifier, a Millipore Milli-Q Plus® system, until the lowest stable integrated area was obtained. Following duplicate seawater sample injections the column was flushed using three injections of 100 μl of Milli-Q water. The catalyst was regenerated using the ''regeneration TC catalyst'' function of the instrument once a week. On average, 25 samples were made daily and the top 2 cm of the catalyst was replaced with fresh material every 2 weeks.

[12] Standardization was carried out every day using freshly prepared potassium hydrogen phthalate (Kanto Chemical Company, Inc.) dissolved in Milli-Q water. The instrument response factor, measured as the slope of the standard addition to Milli-Q ($r^2 > 0.999$ for 19 runs), remained relatively constant and reproducible over the time of analysis. Results indicated that calibration curves have exhibited little difference in the slope (average slope: 6088 ± 230 area/μM C, n = 24) and intercept (average intercept:

Table 2. Summary of Parameters Obtained From Biodegradation Experiments[a]

	Δ t, days	Integrated BP, μM C for Δt	O_2 Consumption Rate, μ mol O_2 l^{-1} d^{-1}	DOC Removal Rate, μ mol C l^{-1} d^{-1}	BGE, %	DOC Labile, %
Mediterranean waters	4	0.32 ± 0.03	1.24 ± 0.23	1.07 ± 0.18	7 ± 1	6 ± 0.9
Atlantic Jet	3	0.54 ± 0.02	1.27 ± 0.14	1.20 ± 0.11	15 ± 2	5 ± 0.5
Gyre	10	2.33 ± 0.36	1.08 ± 0.13	1.10 ± 0.11	21 ± 3	15 ± 2

[a]Δt corresponds to the incubation time where maximum bacterial production (BP) was obtained. BP is obtained from discrete BP values cumulated over successive time intervals until the BP peak was reached. O_2 consumption rate is estimated as the slope of a linear regression of O_2 decrease with time. Rates of DOC removal, BGE, and percentage of labile DOC (l-DOC) were estimated by the following formulas: DOC removal rate = (O_2 consumption rate × RQ) + (time-integrated BP/Δt), assuming RQ = 0.80; BGE = (time-integrated BP/Δt)/(DOC removal rate) × 100; DOC labile (%) = (DOC removal rate × Δt)/(initial DOC value) × 100. BGE is bacterial growth efficiency. BP errors are time-integrated errors of individual data points whereas O_2 consumption rates standard errors were calculated from the slope coefficients of the linear regression of O_2 decrease with time. Standard errors of the quotients (Z) were determined as follows: SE of $Z = 1/Y^2 (Y^2x^2 + X^2y^2)^{1/2}$, where the quotient $Z = X/Y$, X and Y are means, and x is the standard error of X and Y the standard error of Y.

731 ± 291 area units, n = 24). The accuracy and the system blank of our instrument were determined by the analysis of the reference material (J. H. Sharp, University of Delaware, USA) including Deep Atlantic Water (DAW) and low carbon water (LCW) reference standards. The average DOC concentrations in the DAW and in the LCW reference standards were 45 ± 2 μM C, n = 24 and 10 ± 3 μM C, n = 24, respectively. Carbon levels in the LCW ampoules were similar and often higher than the Milli-Q water produced in our laboratory. The TOC concentration of the samples was calculated by averaging the replicate sample injections, subtracting the average Milli-Q value as the total blank and dividing by the slope of the calibration curve.

2.3. Bacterial Production (BP) Measurements

[13] BP was estimated using the ^{3}H-leucine method [*Kirchman*, 1993] at three representative stations where biodegradation experiments were conducted. [4, 5-^{3}H]-leucine (specific activity 112 Ci mmole-1, Amersham) and unlabeled leucine were added to 20 mL samples giving final concentrations of 1.2 and 19 nM, respectively. Duplicate samples and one formalin-killed blank were incubated in the dark, at in situ temperature (±2°C) for 2 hours, during the linear period of incorporation. After incubation, the samples were fixed with formalin (1% final concentration) and filtered onto a 0.2-μm filter (mixed cellulose ester, MFS type, Advantec). The filter was rinsed three times with 5% TCA and stored frozen. Back in the laboratory, the filters were dissolved in 1 mL ethyl acetate and radioassayed in a Packard 1600 scintillation counter. Leucine uptake was converted to BP based on a conversion factor of 1.5 kg C per mole of incorporated leucine. Further details relating to bacterial production methodology are described by *Van Wambeke et al.* [2000].

2.4. Biodegradation Experiments

[14] For the biodegradation experiments, seawater was immediately filtered under a low vacuum (<50 mm Hg) through 0.2-μm polycarbonate filters (Nuclepore, 47-mm filter diameter) to obtain particle and bacteria free seawater and through 0.8-μm filters (Nuclepore, 47-mm filter diameter) to prepare the bacterioplankton inocula while excluding the predators and photoautotrophs. The filters were prerinsed with 2 L of Milli-Q water followed by 500 mL of seawater before use to minimize DOC contamination as suggested by *Yoro et al.* [1999]. The 0.2-μm filtrate (4 L) was inoculated with 1 L of the 0.8-μm solution and then dispensed in duplicate into several Pyrex precombusted (450°C, 6 hours) bottles for the determination of BP and into triplicate 100-ml Winkler bottles for oxygen determinations. For each experiment, killed controls were made by the addition of $HgCl_2$ (final concentration: 10 mg L^{-1}) and analyzed at the end of the experiment. The oxygen bottles were submerged until analysis to minimize gas exchange.

[15] For both experiments, the experimental bottles and controls were incubated in the dark in a temperature controlled room (±1°C) over course of the experiment. Samples were analyzed for BP using a time series of 0, 0.5, 1, 2, 3, 4, and 10 days. Samples for the determination of dissolved oxygen were fixed with Winkler reagents and measurements were made using an automated Winkler titration system based on that described by *Williams and Jenkinson* [1982]. Dark bacterial respiration rates were calculated assuming a linear regression model on the decrease in dissolved oxygen concentration over the time series. For BP, we used the same method as used for natural samples: 20 mL of sample was incubated 2 hours with 20 nM leucine final concentration. Bacterial growth efficiencies (BGE), percentage of labile dissolved organic carbon (l-DOC), and DOC consumption rates were calculated at the BP peak (Table 2) and assumed an averaged respiratory quotient (RQ) of 0.80 taken as an average from literature [*Redfield et al.*, 1963; *Takahashi et al.*, 1985; *Minster and Boulahdid*, 1987; *Lehninger et al.*, 1994; *Shaffer*, 1996, and references therein] in order to convert O_2 respiration rates in terms into CO_2 production. Parameters related to bacterial activity were calculated assuming a linear model for O_2 decrease, and from trapezoidal time-integrated BP using the discrete data of BP over time. BGE, which is the result of BP and bacterial respiration (BR), and bacterial carbon demand (BCD), can be described by the following:

$$\mathrm{BGE} = \mathrm{BP}/(\mathrm{BP} + \mathrm{BR}) \quad (1)$$

$$\mathrm{BCD} = \mathrm{BP} + \mathrm{BR}. \quad (2)$$

2.5. Primary Production Determination

[16] Primary production was calculated according to *Morel et al.* [1996]. Photosynthetic parameters of the P versus I curves were determined, after inoculation with inorganic ^{14}C and incubation at different light intensities using a radial photosynthetron [*Babin et al.*, 1994]. Because

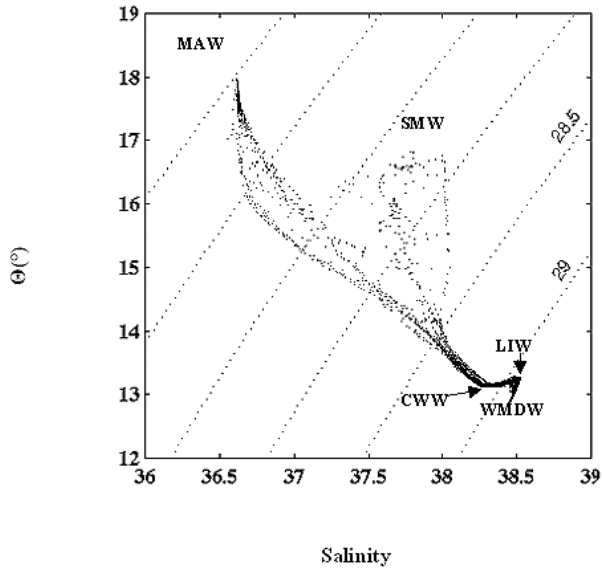

Figure 2. Potential temperature-salinity (Θ -S) diagrams drawn from CTD-rosette casts (every 5 m) between 0 and 1000 m. MAW: Modified Atlantic Water; SMW: Surface Mediterranean Water; LIW: Levantine Intermediate Water; CWW: Cold winter water. WMDW: Western Mediterranean Deep Water.

of the short incubation period (2 hours), we will assume little DOC excretion by the primary producers. Estimation of chlorophyll specific photosynthetical efficiency, α^B (mg C (mg chl a)$^{-1}$ h^{-1} (μmol quanta m^{-2}s^{-1})$^{-1}$), and maximum chlorophyll specific carbon fixation rate (P^B_{max} (mg C (mg chl a)$^{-1}$ h^{-1})) was achieved by adjusting the raw data of carbon fixation and illumination according to the relation of *Platt et al.* [1980]. Calculation of the integrated amount of carbon fixed was carried out over 1.5 times the euphotic depth.

3. Results

3.1. Hydrology

[17] The hydrology during Almofront 2, winter 1997 was similar to the situation described for Almofront 1 in Spring 1991 [*Prieur et al.*, 1993], despite inverse winter temperature distribution typical of winter seasons; that is, Mediterranean waters were warmer than Atlantic waters during Almofront 1. The potential temperature (Θ)-salinity (S) diagram (Figure 2) indicates the presence of surface Mediterranean water (SMW: S ∼ 37.8; Θ ∼ 16.80°C) located near the Spanish coast. In the middle at the southern part of the transect, Θ -S diagrams enabled us to identify modified Atlantic water (MAW: S ∼ 36.62) flowing from the Gibraltar Strait. Below 500 m, water is a combination of Levantine Intermediate Water (LIW: S ∼ 38.47; Θ ∼ 13.25 °C), Cold Winter northwestern Mediterranean Water (CWW: S ∼ 38.35; Θ ∼ 13.15°C) and Deep Western Mediterranean Water (WMDW: S ∼ 38.41; Θ ∼ 12.75°C) [*Parrilla and Kinder*, 1987].

[18] The most striking feature of the area studied is a strong temperature/salinity/density gradient within 50 km from the cold and salty Mediterranean waters to the warmer, less saline and less dense Atlantic waters (Figure 3). The interaction between MAW and SMW produced an extremely strong halocline, which induces a pycnocline and horizontal frontal zone in the AOF whose orientation is normally northwest to southeast [*Tintoré et al.*, 1988]. The density field is therefore mainly influenced by the strong pycnocline around the isopycnal 27.5 kg m^{-3}, whose depth changed from 30 m in Mediterranean waters to ∼200 m inside the modified Atlantic water eddy so forming a well defined interface between Atlantic and Mediterranean waters [*Prieur et al.*, 1993]. The horizontal density gradient (1 kg m^{-3} over 30 km) induces a surface gradient of geopotential (8 dyn cm) and the geostrophic jet, which flows with a velocity as high as 0.80 m s^{-1} at its core (Figure 3a).

[19] Water masses identification, ADCP measurements, and associated calculations indicated that Mediterranean water with specific physical characteristics circulating westward then eastward (0.45 Sv) were concentrated in the area of stations 252–261 (Figure 3a). The core of the Atlantic Jet water circulating (1.2 Sv) toward the eastern Mediterranean Sea was located between stations 262 and 266. The core of the jet, with a geostrophic velocity (within the upper 100 m) as high as 80 cm s^{-1} was found around station 264 (Figure 3a). The dynamic conditions forces the northern part of the gyre to flow eastward (stations 267–269) and recirculate 2.1 Sv relatively warm fresh waters of modified Atlantic water. The center of the anticyclonic Atlantic gyre was identified in the area of stations 270–272. The end of section 272–275 corresponds to the southern flow of the gyre and flowed westward by 2.1 Sv.

3.2. TOC Distribution

[20] The vertical distribution of TOC during leg 1 along the transect shows elevated concentrations in surface waters (0–200 m) ranging from 54 to 107 μM and lower values 45 to 67 μM, below 200 m (Figure 3b). Significant mesoscale variability was particularly evident across the AOF. It is clear that many of the variations observed in the TOC pool co-varied with changes in isohaline depth and velocity of the current (Figures 3a and 3b). This feature was particularly evident within the Atlantic Jet (section 262–266) where low TOC concentrations were concomitant with high current velocities (Figures 3a and 3b). Low TOC concentrations were also observed in the central gyre (section 270–272) whereas the higher TOC concentrations occurred in Mediterranean waters, on the northern flow of the gyre (section 267–269) and near the Algerian coast (section 273–275).

[21] TOC concentrations decreased with depth all along the transect. Excess-TOC between 0 and 100 m, which represents the sum of semi-labile-TOC and labile-TOC was calculated as the difference between discrete surface values and refractory TOC (53 ± 4 μM) estimated from an average of TOC discrete values between 400 and 1000 m (Table 1; Figure 4). Basically, excess-TOC stock accounted for 21 ± 4% (four stations) in the Atlantic Jet, whereas these fractions were 28 ± 2% (six stations) and 28 ± 5% (four stations) in the gyre and Mediterranean waters, respectively. It is important to note that lower ratios (21%) were found in the central gyre (two stations). Clearly, there is a depletion of excess-TOC stocks in the Atlantic Jet and the central gyre whereas there is an accumulation of excess-TOC in the

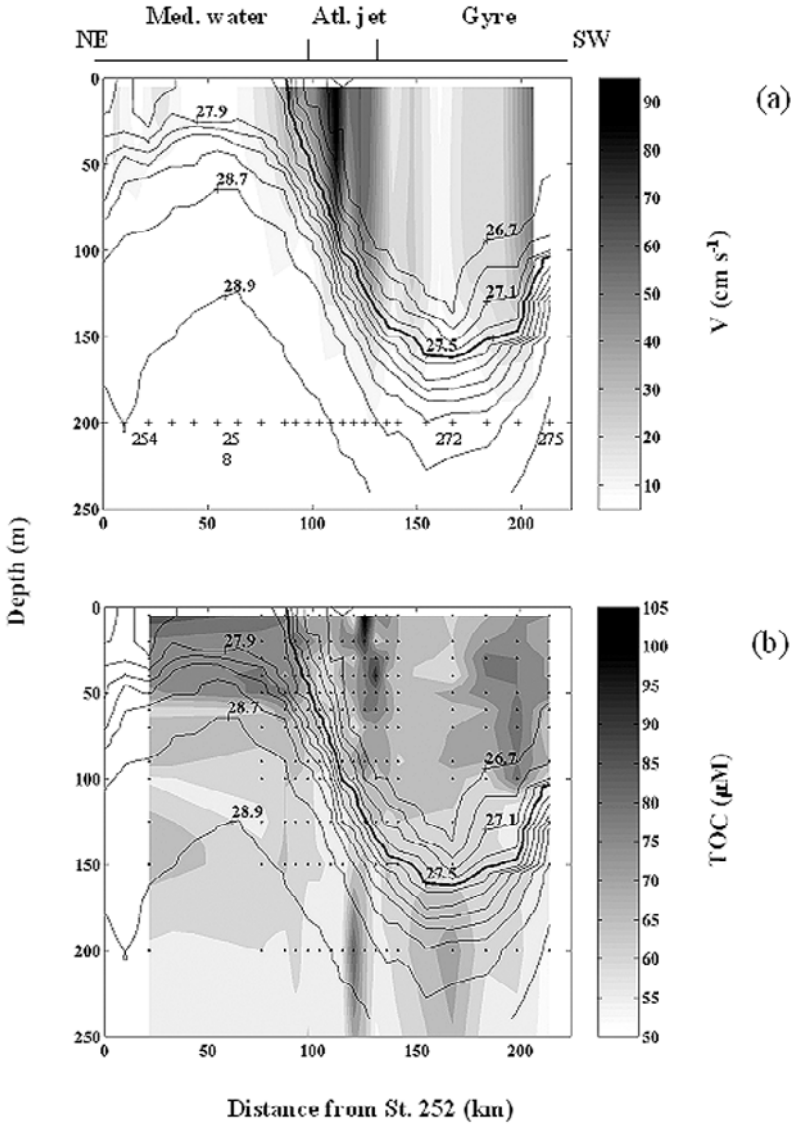

Figure 3. Contour plots of (a) ADCP current geostrophic velocities (cm s^{-1}) and (b) TOC concentrations (μM) with density excess (sigma-theta (kg m^{-3})) calculated from all 5-m CTD- rosette data. The density excess line 27.5 (kg m^{-3}) separates the Mediterranean and Atlantic waters. Numbers (252–275) are station identification numbers.

northern flow of the gyre and to a less extent in the frontal zone between the Mediterranean water and the Atlantic Jet (Figure 4).

3.3. Bacterial Growth on Labile DOC (l-DOC)

[22] The different sources of water support bacterial growth to similar degrees. Oxygen decreased linearly during the biodegradation experiments, with values ranging from 1.08 ± 0.13 to 1.27 ± 0.14 μmol O_2 L^{-1} d^{-1} while BP increased exponentially following a time lag, and reached a maximum after 4, 3, and 10 days using typical Mediterranean waters, Atlantic, and gyre samples, respectively (Table 2). These results indicate that when BP peaked, the fractions of DOC consumed were 6 ± 0.9%, 5 ± 0.5% and 15 ± 2% in Mediterranean, Atlantic Jet, and gyre waters, respectively (Table 2). The removal rates of DOC during the experiments (Table 2) were similar (1.07 ± 0.18 – 1.20 ± 0.11 μmole C L^{-1} d^{-1}) for the three water types. On the other hand, the experimental approach used in this study yielded BGE ranging from 7 ± 1% (Mediterranean water) to 21 ± 3% (gyre, Table 2). Note that according to the RQ selected from the literature [*Redfield et al.*, 1963; *Takahashi et al.*, 1985; *Minster and Boulahdid*, 1987; *Lehninger et al.*, 1994; *Shaffer*, 1996, and references therein], BR and DOC removal rates might be affected by nearly 46%.

3.4. Primary and Bacterial Productions (PP and BP)

[23] BP values measured during leg1, showed little variations in the environments studied (Table 3). Average of PP integrated over the euphotic layer was lower in Mediterranean waters (section 252–258: 9.80 ± 5.9 mmol C m^{-2} d^{-1}) than in the modified Atlantic Jet, (section 262–266: 20.2 ±

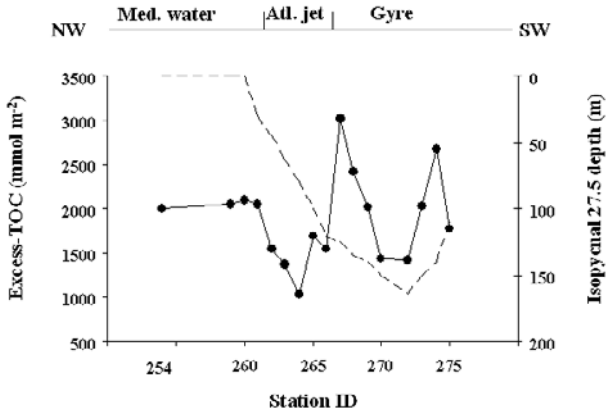

Figure 4. Excess-TOC inventory stocks (mmol C m^{-2}) in the upper 0–100 m. The depth of the density excess line 27.5 kg m^{-3} (dashed line) indicates the depth of the limit between Mediterranean and Atlantic water masses. Integrated excess-TOC was calculated as the integration of the difference between discrete of TOC data in the upper layer and a 200- to 1000-m averaged TOC value (53 μM).

2.2 mmol C m^{-2} d^{-1}), and gyre (section 270–271: 20.0 ± 1.6 mmol C m^{-2} d^{-1}). Marked differences in BP and PP were evident across the AOF; that is, integrated BP/PP ratios over the euphotic layer were highest in the Mediterranean waters (0.43 ± 0.26), followed by the Atlantic Jet (0.20 ± 0.02) and gyre (0.10 ± 0.01) waters. Leg 1 stations were studied consecutively along the transect. However, between leg 1 and leg 2 of the cruise, the meander-gyre system moved eastward. Consequently leg 2 stations were relocated like in the idealized jet-gyre structure as if they had been all studied simultaneously; then it is rather difficult to accurately compare leg 1 and leg 2 stations. Nevertheless, results taken from a limited number of "long station" observations during leg 2 [*Van Wambeke et al.*, 2003] indicated that BP/PP ratios ranged from 0.22 to 0.43 in Mediterranean Seawaters, whereas this ratio ranged from 0.12 to 0.13 in the jet core and from 0.11 to 0.24 around the gyre. These results showed higher BP/PP in the Mediterranean Sea compared to other stations.

4. Discussion

4.1. TOC Concentrations Across the AOF

[24] Our results showed TOC values ranging from 55 μM to 80 μM in surface waters decreasing to 45 μM at 1000 m. These results agree with previous studies dealing with DOC distribution in the Mediterranean Sea [*Copin-Montégut and Avril*, 1993; *Gasol et al.*, 1998; *Doval et al.*, 1999; *Cauwet et al.*, 1997; *Dafner et al.*, 2001b; *Sempéré et al.*, 2002; *Avril*, 2002; *Bianchi et al.*, 2003]. Slightly lower concentrations have been reported for "old" deep DOC in LIW (38–52 μM) at the Gibraltar Strait [*Dafner et al.*, 2001a]. In surface waters, the more striking feature of TOC distribution is the large variability of TOC concentrations within a few kilometers across the AOF; that is, there is TOC accumulation in Mediterranean waters near the Atlantic Jet (frontal zone) and in the northern flow of the gyre, where we found high primary productions (28.2 and 46.3 mmol C m^{-2}, respectively) whereas there is TOC depletion in the Atlantic Jet, which is an area of lower primary production (20.2 mmol C m^{-2}).

4.1.1. Labile-DOC (l-DOC)

[25] Our biodegradation experiments showed that 5 ± 0.5–15 ± 2% of the DOC in surface water is biologically labile and could be exhausted by bacteria within a few days (Table 2), thus being consistent with current knowledge of l-DOC [*Carlson*, 2001]. BGE we found ranged from 7 ± 1 to 21 ± 3% and is consistent with that found for other marine systems [*del Giorgio et al.*, 1997; *Rivkin and Legendre*, 2001; *Carlson*, 2001]. Low values were reported (4–19%) in the Sargasso Sea [*Hansell et al.*, 1995; *Carlson and Ducklow*, 1996] whereas higher BGE range (25–30%) were found by *Kähler et al.* [1997] in the Southern Ocean. Although DOC consumption rates were similar, the variations we observed for BGE between different biodegradation experiments suggested the quality of the utilizable l-DOC and the physiological status of bacterial assemblage varied according to its position across the AOF system.

4.1.2. Excess-TOC

[26] Excess-TOC was estimated as the difference between discrete data and refractory TOC. This TOC consists of semi-labile material turning-over on a seasonal timescale and other less degradable fractions [*Anderson and Williams*, 1999; *Carlson et al.*, 2000; *Carlson*, 2001]. These calculations indicate that there is little excess-TOC accumulated in the Atlantic Jet (21 ± 3%) compared to surrounding waters (up to 32%) (Table 1). Results obtained from the leg 2 study in the same area [*Van Wambeke et al.*, 2003] indicated that particulate organic carbon make up less than 10% of the TOC in the gyre and between 5 and 7% of TOC in Mediterranean Seawaters and in the jet and then there is little variation between the typical sites studied. Thus we feel that the results presented will not be affected greatly by suspended POC. Other studies have calculated that excess-DOC accounts for 18–40% of the DOC [*Carlson et al.*,

Table 3. Integrated Bacterial Production (BP: 0–100 m) and Excess-TOC Residence Time[a]

Stations	BP, mmol C m^{-2} d^{-1}	Value of BGE Used, %	Excess-TOC Residence Time, days	Excess-TOC Residence $Time_{0.24}$, days
Mediterranean waters	5.1	7	28 ± 1	96 ± 2
Modified Atlantic Jet	5.2	15	42 ± 7	65 ± 13
Gyre	4.1	21	109 ± 30	124 ± 34

[a]Average residence times for different water types are given by excess-TOC/BP/BGE and for comparison, with a mean value of 24% [*del Giorgio et al.*, 1997]. Excess-TOC and BP are integrated values over the layer 0–100 m. BGE were taken from biodegradation experiments; the same BP and BGE were used for all the gyre. Excess-TOC residence times are averages of the different stations studied along the transect (see Table 1) with a standard deviation calculated from the variation of the TOC concentrations and the water transport.

1994; *Carlson and Ducklow*, 1995; *Wiebinga and de Baar*, 1998; *Kähler and Koeve*, 2001; *Sempéré et al.*, 2002], the lowest values being reported for the Sargasso Sea (20% [*Carlson et al.*, 1994]), southern Aegean Sea [*Sempéré et al.*, 2002], and the Southern Ocean [*Wiebinga and de Baar*, 1998; *Ogawa et al.*, 1999].

4.2. Utilization of TOC in the AOF System

[27] Because DOC is a by-product of primary production and is essentially consumed by bacteria, our results indicate large balance variability across the AOF between TOC production by primary production derived processes and its utilization by bacteria. Interestingly, the results indicate that Mediterranean waters are characterized by a low l-DOC pool (6 ± 0.9%), high excess-TOC (28 ± 0.4%), low PP, and high BP/PP ratios. Taking into consideration PP, BP, and BGE measured simultaneously during the cruise, the ratio of BCD to PP was largely greater than 100% in Mediterranean waters whereas this proportion was lower in the AOF system. Applying the general value of 24% [*del Giorgio et al.*, 1997] infers that local, instantaneous PP is not sufficient to supply BCD in the Mediterranean site probably because of a delay between photosynthetic DOC production and its consumption by heterotrophic bacteria. Low PP in relation to BCD and bacterial respiration (BR) exceeding PP have been reported already for western Mediterranean Sea [*Turley et al.*, 2000]. Excess-TOC levels in these waters might be explained by the accumulation of recalcitrant organic compounds due to rapid diagenetic processes governed by microorganisms [*Ogawa et al.*, 2001] and/or to phosphorus deficiency, which gives rise to lower bacterial activity [*Van Wambeke et al.*, 2003].

[28] Despite the high values found for integrated PP at the edges of the Atlantic Jet and in the gyre waters, there are only small amounts of l-DOC (5 ± 0.5%) and semi-labile TOC (20 ± 3%) accumulating in the Atlantic Jet waters whereas these fractions are more abundant within the gyre (15 ± 2% and 28 ± 6%). Because the BP/PP ratios were higher in the jet (0.20) than in the gyre (0.10), these results suggest a more efficient coupling between primary and bacterial productions in the jet than in the gyre although this feature was not observed during leg 2 [*Van Wambeke et al.*, 2003]. Intermediate values found for l-DOC and the BP/PP ratios suggest that BP-PP coupling is not the only process governing l-DOC distribution in the Atlantic Jet.

[29] Note that secondary circulation may contribute to the exchange of surface Atlantic Jet waters and intermediate waters [*Prieur and Sournia*, 1994]. Indeed, it has been indicated [*Lohrenz et al.*, 1988; *Videau et al.*, 1994] that the advection of upwelled water, which is rich in nutrients, into the photic zone ($1-2$ m d^{-1}) enhances PP and probably TOC production near the jet in the frontal zone. The resulting TOC-rich waters may then be downwelled by the convergent part of the ageostrophic circulation along the isopycnals as shown for chlorophyll and other pigments [*Claustre et al.*, 1994; *Videau et al.*, 1994]. These trends can not be fully evidenced in the AOF because TOC is not a conservative parameter. However, the large variability of TOC concentration that we observed for the first time in such frontal structure at mesocale level is very likely due to the input of nutrients into surface waters and to the subsequent increase of primary production as well as to the downwelling of surface water on the edges of the front. Such processes are very likely to occur in other frontal structures.

[30] In the jet and gyre, integrated BP comprises 20% and 10% of the PP, so that 131% and 48% of PP may be routed through the DOC reservoir and support the BCD (Table 3) indicating that bacteria are strongly dominating the food web within the jet. By using the experimental BGE estimated during this study, our results indicated that in the Atlantic Jet, bacterial respiration (BR: 34.7 mmol C m^{-2} d^{-1}) is higher than PP (20.2 mmol C m^{-2} d^{-1}) suggesting that during the period studied, the jet could be regarded as an heterotrophic system and a net source of CO_2. On the other hand, in the gyre, PP (20.0 mmol C m^{-2} d^{-1}) is similar to BR (19.5 mmol C m^{-2} d^{-1}) suggesting that the biological system reached an equilibrium during the cruise. However, there are large uncertainties associated to such calculations (particularly those associated with BGE calculations), and these calculations can not be extended to longer timescales in the AOF system.

[31] Assuming that equal BGE could be used for l-DOC and semi-labile-TOC and by using BP values at the three typical leg 1 stations, we can estimate that excess-TOC would be exhausted in 28 ± 1 days in Mediterranean waters, 42 ± 7 days in the Atlantic Jet, and in 109 ± 30 days in the gyre (Table 3). The use of a constant, theoretical BGE of 24% in all data [*del Giorgio et al.*, 1997] gives only an increase in excess-TOC residence times and then does not change the general pattern of excess-TOC in the area studied and indicates rapid cycling of the most labile part of TOC in the Atlantic Jet compared to the gyre. Such bacterial utilization of TOC within the geostrophic front is likely to minimize large exportation of TOC from the western toward the eastern Mediterranean Sea.

[32] Excess-TOC residence times based on water column BP measurements range from less than one month for the Polar Frontal Zone [*Kähler et al.*, 1997] and the South Aegean Sea [*Sempéré et al.*, 2002] to more than 1 year for the Arctic Ocean [*Wheeler et al.*, 1996]. Studies based on a seasonal water column DOC survey, indicate large variations ranging from less than two months in the Ross Sea [*Carlson et al.*, 2000] to more than 1 year in the northwestern Mediterranean Sea [*Copin-Montégut and Avril*, 1993] and the Sargasso Sea [*Hansell et al.*, 1995]. Excess-TOC residence time based on integrated DOC/TOC stocks and instantaneous BP rates are probably underestimated in our study because instantaneous BP do not reflect growth supported by recalcitrant material, which is present in excess-TOC [*Carlson*, 2001].

4.3. TOC Transport in the AOF System

[33] The Atlantic water jet core flow was calculated to be 1.2 Sv. Applying the TOC data from this study, this value of water transport will yield a TOC transport by the geostrophic jet of $8.04 \pm 0.32 \times 10^4$ mol C s^{-1}, which is higher than the Atlantic Ocean input calculated at the Gibraltar Strait one 160 km to the West, in spring 1998 (TOC: 4.80×10^4 mol C s^{-1} [*Dafner et al.*, 2001a]) and in autumn 1997 (TOC: 7.30×10^4 mol C s^{-1} [*Dafner et al.*, 2001b]). This difference is due to TOC concentrations and to water transport variability since these authors measured an Atlantic inflow of 0.80 Sv at the western entrance of the Strait, whereas examination of other studies indicates large

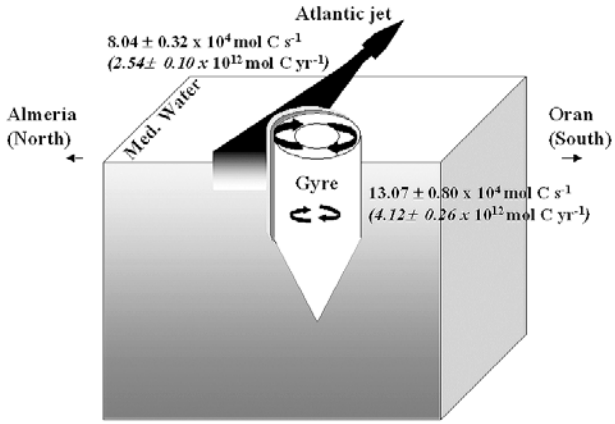

Figure 5. Sketch of the Atlantic Jet in the Alboran Sea with the Atlantic Anticylonic Gyre based on TOC transport calculated from an average of TOC concentration in the upper 100 m for the jet and the upper 200 m for the gyre and by using ADCP current velocities. Numbers in italics are related to an annual estimate. Errors are related to the variations of TOC and water transport measured along the transect.

variability in the Atlantic inflow ranging from 0.68 to 2 Sv [*Lacombe and Richiez*, 1982; *Béthoux*, 1980; *Bryden and Kinder*, 1988; *Tsimplis and Bryden*, 2000]. During the Almofront 1 cruise in the Alboran Sea (spring 1991), similar eastward jet transport was reported with a weaker gyre circulation (0.80 Sv). Surface TOC values reported here are slightly higher than those found in the Atlantic inflow in spring probably as a consequence of coastal upwelling and the associated increasing productivity in the Alboran Sea near the Spanish coast [*Dafner et al.*, 2001b]. Finally, the increase in productivity observed in the AOF contributes to the organic content of the geostrophic jet.

[34] Over a year, the TOC input within the jet would be around $2.54 \pm 0.10 \times 10^{12}$ mol C yr^{-1} (Figure 5). Taking into account the variability of the water inflow ranging from 0.68 to 2 Sv [*Lacombe and Richiez*, 1982; *Béthoux*, 1980; *Bryden and Kinder*, 1988; *Tsimplis and Bryden*, 2000], the TOC transport of the Atlantic Jet would range from 1.44 ± 0.06 to $4.23 \pm 0.17 \times 10^{12}$ mol C yr^{-1}. The results indicate that TOC transport within the jet core is one order of magnitude higher than Mediterranean river discharge [*Ludwig et al.*, 1998; *Sempéré et al.*, 2000], atmospheric deposition [*Loyë-Pillot et al.*, 1992; *Copin-Montégut*, 1993] or Black Sea inputs (*Polat and Tugrul*, 1996; *Sempéré et al.*, 2002). The TOC transport within the gyre would average $13.07 \pm 0.80 \times 10^4$ mol C s^{-1}. This highlights that the gyre is an area where a large quantity of organic carbon is circulating anticyclonically being locally fuelled and consumed by the autotrophic and heterotrophic organisms.

5. Summary and Conclusion

[35] This study highlights significant TOC variability in surface waters driven by the different functioning of the microbial food web within a few kilometers and indicates that a mesoscale approach is necessary for use in biogeochemical studies. This is particularly evident in highly contrasting systems with frontal structures. We found that TOC dynamics in the gyre will change the amplitude of the seasonal CO_2 exchange with the atmosphere locally in the Alboran Sea. We can expect that exported TOC from the surface layer within the Atlantic Jet will ultimately be mineralized to CO_2 in the eastern part of the South Mediterranean Sea. Such coupling between horizontal water mass transport and bacterial cycling of semi-labile TOC is likely to be an important process in other "highly" dynamic oceans such as the Antarctic Ocean where circumpolar circulation probably exports large amount of semi-labile TOC ready for the subsequent CO_2 production *via* bacterial respiration and thus needs to be taken into account in the construction of global carbon cycle models.

[36] **Acknowledgments.** The authors appreciated the critical comments on the draft provided by A. Bianchi, B. Charrière, and Imma Tholosa and those given by anonymous reviewers. We appreciated the English correction of the manuscript made by Tracy Bentley. We thank the officers and crew of the RV *L'Atalante* for their valuable assistance and support as well as J. Raunet and D. Tailliez for CTD cast operations and M. Pujo-Pay for help during biodegradation experiments onboard. This research was funded by the Almofront2/JGOFS program in the framework of PROOF project from CNRS/INSU France. Financial support for E. Dafner came from Ministère des Affaires Etrangères Français and Conseil Général des Bouches du Rhône, France. This article is contribution 268 from the Center for Marine Sciences, (UNCW) USA, for E. D.

References

Anderson, T. R., and P. J. L. B. Williams, A one-dimensional model of dissolved organic carbon cycling in the water column incorporating combined biological-photochemical decomposition, *Global Biogeochem. Cycles*, *13*, 337–349, 1999.

Arnone, R. A., D. A. Wiesenbourg, and K. D. Saunders, The origin and characteristics of the Algerian current, *J. Geophys. Res.*, *95*, 1587–1598, 1990.

Avril, B., DOC dynamics in the northwestern Mediterranean Sea (Dyfamed Site), *Deep Sea Res.*, *Part II*, *49*, 2163–2182, 2002.

Babin, M., A. Morel, and R. Gagnon, An incubator designed for extensive and sensitive measurements of phytoplankton photosynthetic parameters, *Limnol. Oceanogr.*, *39*, 694–702, 1994.

Baldacci, A., G. Corsini, R. Grasso, G. Manzella, J. T. P. Allen, P. Cipollini, T. H. Guymer, and H. M. Snaith, A study of the Alboran sea mesoscale system by means of empirical orthogonal function decomposition of satellite data, *J. Mar. Syst.*, *29*, 293–311, 2001.

Béthoux, J. P., Mean water fluxes across sections in the Mediterranean Sea evaluated on the basis of water and salt budgets and observed salinities, *Oceanol. Acta*, *3*, 79–88, 1980.

Bianchi, A., et al., Microbial activity at the deep water sediment boundary layer in two highly productive systems in the western Mediterranean: The Almeria-Oran front and the Malaga upwelling, *Oceanol. Acta*, *25*, 315–324, 2003.

Bryden, H. L., and T. H. Kinder, Gibraltar experiment: A plan for dynamic and kinematic investigations of strait mixing, exchange and turbulence, in *Pelagic Mediterranean Oceanography*, edited by H. J. Minas and P. Nival, *Oceanol. Acta, NSP 9*, 29–40, 1988.

Carlson, C. A., DOM production and consumption, in *Biogeochemistry of Marine Dissolved Organic Matter*, edited by D. A. Hansell and C. A. Carlson, pp. 91–151, Academic, San Diego, Calif., 2001.

Carlson, C. A., and H. W. Ducklow, Dissolved organic carbon in the upper ocean of the central Pacific Ocean, 1992: Daily and finescale vertical variations, *Deep Sea Res.*, *Part II*, *42*, 639–656, 1995.

Carlson, C. A., and H. W. Ducklow, Growth of bactrioplankton and consumption of dissolved organic carbon in the Sargasso Sea, *Aquat. Microbial. Ecol.*, *10*, 69–85, 1996.

Carlson, C. A., H. W. Ducklow, and A. F. Michaels, Annual flux of dissolved organic carbon from the euphotic zone in the northwestern Sargasso Sea, *Nature*, *371*, 405–408, 1994.

Carlson, C. A., D. A. Hansell, E. T. Peltzer, and W. O. Smith, Stocks and dynamics of dissolved and particulate organic matter in the southern Ross Sea, Antarctica, *Deep Sea Res.*, *Part II*, *47*, 3201–3225, 2000.

Cauwet, G., HTCO method for dissolved organic carbon analysis in seawater: Influence of catalyst on blank estimation, *Mar. Chem.*, *47*, 55–64, 1994.

Cauwet, G., A. Miller, S. Brasse, G. Fengler, R. F. C Mantoura, and A. Spitzy, Dissolved and particulate organic carbon in the western Mediterranean Sea, *Deep Sea Res.*, *Part II*, *44*, 769–779, 1997.

Claustre, H., P. Kerhervé, J. C. Marty, and L. Prieur, Phytoplankton photoadaptation related to some frontal physical processes, *J. Mar. Syst.*, *5*, 251–265, 1994.

Claustre, H., F. Fell, K. Oubelkeir, L. Prieur, A. Sciandra, B. Gentili, and M. Babin, Continous monitoring of surface optical properties across a geostrophic front: Biogeochemical inferences, *Limnol. Oceanogr.*, *45*, 309–321, 2000.

Copin-Montégut, C., Alkalinity and carbon budgets in the Mediterranean Sea, *Global Biogeochem. Cycles*, *7*, 915–925, 1993.

Copin-Montégut, G., and B. Avril, Vertical distribution and temporal variation of dissolved organic carbon in the north-west Mediterranean Sea, *Deep Sea Res.*, *40*, 1963–1972, 1993.

Cussatlegras, A. S., P. Geistdoerfer, and L. Prieur, Planktonic bioluminescence measurements in the frontal zone of Almeria-Oran (Mediterranean Sea), *Oceanol. Acta*, *24*, 239–250, 2001.

Dafner, E. V., R. Sempéré, F. González, F. Gomez, and M. Goutx, Cross-slope variations of dissolved organic carbon in the Gulf of Cadiz in relation to water dynamics (February 1998), *Mar. Ecol. Prog. Ser.*, *189*, 301–306, 1999.

Dafner, E. V., R. Sempéré, and H. Bryden, Total organic carbon distribution through the Strait of Gibraltar in September 1997, *Mar. Chem.*, *73*, 233–252, 2001a.

Dafner, E. V., M. González-Dávila, J. M. Santana-Casiano, and R. Sempéré, Total organic and inorganic carbon exchange through the Strait of Gibraltar in September 1997, *Deep Sea Res.*, *Part I*, *48*, 1217–1235, 2001b.

del Giorgio, P. A., J. J. Cole, and A. Cimbleris, Respiration rates in bacteria exceed phytoplankton production in unproductive aquatic systems, *Nature*, *385*, 148–151, 1997.

Doval, M. D., F. Pérez, and E. Berdalet, Dissolved and particulate organic carbon in the northwestern Mediterranean Sea, *Deep Sea Res.*, *Part I*, *46*, 511–527, 1999.

Fernàndez, M., M. Bianchi, and F. Van Wambeke, Bacterial biomass, heterotrophic production and utilization of dissolved organic matter photosynthetically produced in the Almeria-Oran front, *J. Mar. Syst.*, *5*, 313–325, 1994.

Gasol, J. M., M. D. Doval, J. Pinhassi, J. I. Calderón-Paz, N. Guixa-Boixareu, D. Varque, and C. Pedrós-Alió, Diel variations in bacterial heterotrophic activity and growth in the north-western Mediterranean Sea, *Mar. Ecol. Prog. Ser.*, *164*, 107–124, 1998.

Grout, H., R. Sempéré, A. Thill, A. Calafat, L. Prieur, and M. Canals, Morphological and chemical variability of colloids in the Almeria-Oran Front in the eastern Alboran Sea (SW Mediterranean Sea), *Limnol. Oceanogr.*, *46*, 1347–1357, 2001.

Hansell, D. A., DOC in the global carbon cycle, in *Biogeochemistry of Marine Dissolved Organic Matter*, edited by D. A. Hansell and C. A. Carlson, pp. 685–715, Academic, San Diego, Calif., 2001.

Hansell, D. A., N. R. Bates, and K. Gundersen, Mineralization of dissolved organic carbon in the Sargasso Sea, *Mar. Chem.*, *51*, 201–212, 1995.

Kähler, P., and W. Koeve, Marine dissolved organic matter: Can its C:N ratio explain carbon overconsumption?, *Deep Sea Res.*, *Part I*, *48*, 49–62, 2001.

Kähler, P., P. K. Bjørnsen, K. Lochte, and A. Antia, Dissolved organic matter and its utilisation by bacteria during spring in the Southern Ocean, *Deep Sea Res.*, *Part II*, *44*, 341–353, 1997.

Kirchman, D. L., Leucine incorporation as a measure of biomass production by heterotrophic bacteria, in *Handbook of Methods in Aquatic Microbial Ecology*, edited by P. F. Kemp et al., pp. 509–512, Lewis, New York, 1993.

Lacombe, H., and C. Richiez, The regime of the Strait of Gibraltar, in *Hydrodynamics of Semi-Enclosed Seas*, edited by J. C. J. Nihoul, pp. 13–74, Elsevier Sci., New York, 1982.

La Violette, P. E., The Western Mediterranean Circulation Experiment (WMCE): Introduction, *J. Geophys. Res.*, *95*, 1511–1514, 1990.

Lehninger, A. L., D. L. Nelson, and M. M. Cox, *Principes de Biochimie*, 2nd ed., 1035 pp., Flammarion, Paris, 1994.

Lohrenz, S. E., D. A. Wisenbourg, I. P. De Palma, K. S. Johnson, and D. E. Gustafson, Interrelationships among primary production, chlorophyll, and environmental conditions in the frontal regions of the western Mediterranean Sea, *Deep Sea Res.*, *35*, 793–810, 1988.

Loyë-Pillot, M. D., G. Cauwet, A. Spitzy, and J. M. Martin, Preliminary results on atmospheric wet deposition of organic carbon and nitrogen in Corsica, in *EROS 2000, Third Workshop on the North-West Mediterranean Sea, Den Burg-Texel, 21,025 October 1991*, edited by J. M. Martin and H. Barth, *Water Pollut. Res. Rep.*, *28*, pp. 519–532, Comm. of the Eur. Comm., Brussels, 1992.

Ludwig, W., J. L. Probst, and S. Kempe, Atmospheric CO_2 consumption by continental erosion: Present day controls and implications for the last glacial maximum, *Global Planet. Change*, *16–17*, 107–120, 1998.

Minster, J. F., and M. Boulahdid, Redfield ratios along isopycnal surfaces—A complementary study, *Deep Sea Res.*, *Part I*, *34*, 1981–2003, 1987.

Morel, A., D. Antoine, M. Babin, and Y. Dandonneau, Measured and modeled primary production in the northeast Atlantic (EUMELI JGOFS Program): The impact of natural variations in photosynthetic parameters on model predictive skill, *Deep Sea Res.*, *Part I*, *43*, 1273–1304, 1996.

Ogawa, H., and N. Ogura, Comparison of two methods for measuring dissolved organic carbon in sea water, *Nature*, *356*, 696–698, 1992.

Ogawa, H., R. Fukuda, and I. Koike, Vertical distributions of dissolved organic carbon and nitrogen in the Southern Ocean, *Deep Sea Res.*, *Part I*, *46*, 1809–1826, 1999.

Ogawa, H., Y. Amagai, I. Koike, K. Kaiser, and R. Benner, Production of refractory dissolved organic matter by bacteria, *Science*, *292*, 917–920, 2001.

Parrilla, G., and T. Kinder, The physical oceanography of the Alboran Sea, *Bol. Inst. Esp. Oceanogr.*, *4*, 133–165, 1987.

Platt, T. C., C. L. Gallegos, and W. G. Harrison, Photoinhibition of photosynthesis in natural assemblages of marine phytoplankton, *J. Mar. Res.*, *38*, 687–701, 1980.

Polat, Ç., and S. Tugrul, Chemical exchange between the Mediterranean and the Black Sea via the Turkish Straits, in *Dynamics of Mediterranean Straits and Channels, Bull. Inst. Océanogr. Monaco*, *SP 17, CIESM Sci. Ser. 2*, edited by F. Briand, pp. 167–186, Int. Conn. for the Sci. Explor. of the Mediter. Sea, Monaco, 1996.

Prieur, L., and A. Sournia, "Almofront-1" (April–May 1991): An interdisciplinary study of the Almeria-Oran geostrophic front, SW Mediterranean Sea, *J. Mar. Syst.*, *5*, 187–203, 1994.

Prieur, L., C. Copin-Montégut, and H. Claustre, Biophysical aspect of "Almofront 1", an intensive study of a geostrophical front jet, *Ann. Inst. Oceanogr. Monaco*, *69*, 71–86, 1993.

Redfield, A. C., B. H. Ketchum, and F. A. Richards, The influence of organisms on the composition of seawater, in *The Sea*, vol. 2, *The Composition of Sea Water,* edited by M. N. Hill, pp. 26–77, John Wiley, Hoboken, 1963.

Rivkin, R., and L. Legendre, Biogenic carbon cycling in the upper ocean: Effects of microbial respiration, *Science*, *291*, 2398–2400, 2001.

Sempéré, R., B. Charrière, F. Van Wambeke, and G. Cauwet, Carbon inputs of the Rhône River to the Mediterranean Sea: Biogeochemical implications, *Global Biogeochem. Cycles*, *14*, 669–681, 2000.

Sempéré, R., C. Panagiotopoulos, R. Lafont, B. Marroni, and F. Van Wambeke, Total organic carbon dynamic in Aegean Sea, *J. Mar. Syst.*, *33–34*, 355–364, 2002.

Shaffer, G., Biogeochemical cycling in the global ocean: 2. New production, Redfield ratios, and remineralization in the organic pump, *J. Geophys. Res.*, *101*, 3723–3745, 1996.

Takahashi, T., W. S. Broecker, and S. Langer, Redfield ratio based on chemical data from isopycnal surfaces, *J. Geophys. Res.*, *90*, 6907–6924, 1985.

Thibault, D., R. Gaudy, and J. Le Fèvre, Zooplankton biomass, feeding and metabolism in a geostrophic frontal area (Almeria-Oran Front, western Mediterranean): Significance to pelagic food webs, *J. Mar. Syst.*, *5*, 297–312, 1994.

Tintoré, J., P. E. LaViolette, I. Blade, and A. Cruzado, A study of an intense density front in the eastern Alboran Sea: The Almeria-Oran front, *J. Phys. Oceanogr.*, *18*, 1384–1397, 1988.

Tsimplis, M., and H. L. Bryden, Estimation of transport through the Strait of Gibraltar, *Deep Sea Res.*, *Part I*, *47*, 2219–2242, 2000.

Turley, C. M., M. Bianchi, U. Christaki, J. R. W. Harris, S. Psarra, G. Ruddy, E. D. Stutt, A. Tselepides, and F. Van Wambeke, Relationship between primary producers and bacteria in an oligotrophic sea—The Mediterranean and biogeochemical implications, *Mar. Ecol. Prog. Ser.*, *193*, 11–18, 2000.

Van Wambeke, F., U. Christaki, M. Bianchi, S. Psarra, and A. Tselepides, Heterotrophic bacterial production in the Cretan Sea (NE Mediterranean), *Prog. Oceanogr.*, *46*, 205–216, 2000.

Van Wambeke, F., R. Sempéré, M. Bianchi, D. Lefèvre, L. Prieur, and K. Oubelkheir, Bacterioplankton dynamics across a geostrophic front (Almeria-Oran, Southwestern Mediterranean Sea): Physical control on bacterial resources, bacterial grazing and heterotrophic activities, *Mar Ecol. Prog. Ser.*, in press, 2003.

Vazquez-Cuervo, J., J. Font, and J. J. Martinez, Observations on the circulation in the Alboran Sea using ERS 1 altimetry and sea surface temperature data, *J. Phys. Oceanogr.*, *26*, 1426–1439, 1996.

Videau, C., A. Sournia, L. Prieur, and M. Fiala, Phytoplankton and primary production characteristics at selected sites in the geostrophic Almeria-Oran front system (SW Mediterranean Sea), *J. Mar. Syst.*, *5*, 235–250, 1994.

Wheeler, P. A., M. Gosselin, E. Sherr, D. Thibault, D. L. Kirchman, R. Benner, and T. E. Whitledge, Active cycling of the organic carbon in the central Arctic Ocean, *Nature*, *380*, 697–699, 1996.

Wiebinga, C. J., and H. J. W. de Baar, Determination of the distribution of dissolved organic carbon in the Indian sector of the Southern Ocean, *Mar. Chem.*, *61*, 185–201, 1998.

Williams, P. J. le. B., and N. W. Jenkinson, A transportable microprocessor-controlled precise Winkler titration suitable for field station and ship-board use, *Limnol. Oceanogr.*, *27*, 576–584, 1982.

Yoro, S. C., C. Panagiotopoulos, and R. Sempéré, Dissolved organic carbon contamination induced by filters and storage bottle, *Water Res.*, *33*, 1956–1959, 1999.

Youssara, F., and R. Gaudy, Variations of zooplankton in the frontal area of the Alboran Sea (Mediterranean Sea) in winter 1997, *Oceanol. Acta*, *24*, 361–376, 2001.

S. Allègre, M. Bianchi, R. Sempéré, and F. Van Wambeke, Laboratoire de Microbiologie Marine, CNRS/INSU, UMR 6117, Case 907, Centre d'Océanologie de Marseille, Université de la Mediterranée, Campus de Luminy, 13 288 Marseille Cedex 9, France. (m-bianchi@com.univ-mrs.fr; sempere@com.univ-mrs.fr; wambeke@com.univ-mrs.fr)

F. Bruyant and L. Prieur, Laboratoire d'Océanographie de Villefranche, Observatoire Océanologique, INSU/CNRS, ESA 7077, BP 08, *F* 06230 Villefranche-sur-Mer, France. (bruyant@obs-vlfr.fr; prieur@obs-vlfr.fr)

E. Dafner, School of Ocean and Earth Science and Technology, University of Hawaii, Honolulu, HI 96822, USA. (evgeny@hawaii.edu)

D. Lefèvre, Laboratoire d'Océanologie Biologique, CNRS/INSU UMR 6535, Case 901, Centre d'Océanologie de Marseille, Université de la Mediterranée, Campus de Luminy, 13 288 Marseille Cedex 9, France. (lefevre@com.univ-mrs.fr)

C. Magen, Sciences, Université McGill, 3450 Rue University, Montréal, Québec, Canada, H3A 2A7. (cmagen@eps.mcgill.ca)